



Research Article

UTILIZATION OF ORGANIC RANKINE CYCLE FOR ANALYZING ENERGY AND EXERGY OF THE WASTE HEAT RECOVERY SYSTEM

Farzad HOSSAIN*¹, Md. Ashrafuzzaman MIAH²

¹Islamic University of Technology, Department of Mechanical and Production Engineering, Gazipur, BANGLADESH; ORCID: 0000-0001-8256-8553

²Islamic University of Technology, Department of Mechanical and Production Engineering, Gazipur, BANGLADESH; ORCID: 0000-0002-3608-6833

Received: 23.04.2020 Revised: 08.09.2020 Accepted: 20.09.2020

ABSTRACT

The study analyzes exergy and energy by applying environment-friendly newly developed refrigerants. Initially, a thermodynamic model has been developed. Then, not only energy but also exergy have been investigated utilizing the model. Various environment-friendly refrigerants have been selected as working fluids to compare the effects of net work output, pump consumption, coolant flow rate, thermal efficiency, exergy efficiency, exergy destructions, condenser exergy reduction, and exergy efficiencies with various evaporator pressures. It has been found that R141b and R21 give the highest amount of thermal and exergy efficiency at low and high evaporator pressure respectively. Moreover, R141b gives the highest amount of pump consumption and net work output whereas; R124 gives the highest amount of coolant flow rates. Additionally, R141b and R21 refrigerants give the highest amount of evaporator and condenser exergy efficiency respectively. On the contrary, R124 refrigerant gives the highest amount of expander exergy efficiency. In this paper, analysis has been done for various environment-friendly newly developed refrigerants which are very rare in the literature. The paper contributes significant impacts for reducing environmental emissions and improving organic Rankine cycle systems.

Keywords: Energy analysis, exergy analysis, efficiency, organic rankine cycle, evaporator pressure, refrigerant.

1. INTRODUCTION

Energy is a kind of conserved quantity and the concept of energy is based on the first law of thermodynamics. According to the first law of thermodynamics, energy cannot be destroyed or created and it can only be transformed from one form to another. On the other hand, exergy is the available useful energy and the concept of exergy is based on the second law of thermodynamics. According to the second law of thermodynamics, exergy is always destroyed when a process is irreversible.

Domestic and industrial heating utilized around 50% of fuel consumption in most developed countries and a major portion of them is wasted. Usually, low-grade industrial heat is discarded which becomes a major environmental issue due to thermal pollution. To step towards a clean

* Corresponding Author: e-mail: farzadhossain@iut-dhaka.edu, tel: +(880) 1840199782

environment, it is necessary to look for appropriate technologies. Utilizing the organic Rankine cycle, low-grade industrial heat can be converted to electricity which is very efficient and environment friendly.

Yang et al. [1] analyzed performance and presented parametric optimization for diesel engine waste heat recovery system of organic Rankine cycle utilizing fin and tube evaporator and found that the operating conditions of the engine were mostly influencing the optimal evaporation pressures. Nazari et al. [2] proposed a combined steam-organic Rankine cycle (ORC) for recovering the waste heat and found the best performance from exergo-economic and thermodynamic viewpoints by utilizing R152a as working fluid. Yağlı et al. [3] chose R245fa as a working fluid and designed supercritical and subcritical organic Rankine cycle for recovering waste heat of exhaust gas and found better performance in supercritical ORC in comparison to subcritical ORC. Zhai et al. [4] investigated and categorized heat sources of organic Rankine cycle and recommended performance metrics for ORC systems with various heat sources. Sun et al. [5] evaluated the exergy efficiency of ORC-based combined cycles and ORC and found the increment of exergy efficiency at the initial stage but whenever evaporation temperature was increased, the exergy efficiency started decreasing for particular waste heat conditions. Tian et al. [6] examined thermo-economic conditions of zeotropic mixtures utilizing double loop ORC and found that the irreversibility in the evaporator, expander, and internal heat exchanger mainly contributed to the destruction of exergy. Koroglu and Sogut [7] analyzed the marine power plant's waste heat recovery system utilizing the organic Rankine cycle and found that R113 was the best fluid for lower flammability and toxicity and it has the potentiality to improve exergy efficiency. Seyedkavoosi et al. [8] investigated the internal combustion engines' waste heat recovery system utilizing an organic Rankine cycle and revealed that utilizing R-123 as a working fluid gave a comparatively better performance for the chosen conditions. Ge et al. [9] noticed that whenever the condensation dew point temperature of the high-temperature loop increased, it caused a decrement of net power output. Koç et al. [10] found the best performance by utilizing a subcritical regenerative organic Rankine cycle.

Khosravi et al. [11] selected the organic cycle for decreasing system costs and increasing efficiency. Liang et al. [12] noticed that utilizing R1233zd(E) as a working fluid provided the highest net power output. Han et al. [13] realized that the energy recovery requisites of LNG-fueled vessels along with lower cost and higher net output power can be maintained by utilizing novel ORC. Liu et al. [14] noticed the decrement of thermal efficiency with the increment of condenser's outlet temperature. Liao et al. [15] found a higher rate of endogenous exergy in comparison to the exogenous exergy for all of the system components. Hou et al. [16] found the poorest thermodynamic perfection and the highest exergy loss from the condenser and evaporator respectively. Ochoa et al. [17] found higher exergy destruction by utilizing acetone and toluene as working fluids. Wang et al. [18] noticed that operation temperature did not affect the variation characteristics of exergy loss, entransy efficiency, and entropy generation rate whatever be the working fluid. Zhou et al. [19] identified that the superheater area highly affected the evaporating area and the evaporating temperature of the evaporator.

While there are a variety of articles related to energy and exergy analysis of organic Rankine cycle, the majority of them only explored impacts of traditional refrigerants. On the other hand, the paper investigated exergy and energy by applying environment-friendly newly developed refrigerants which is rare in the literature. Besides, it can be worth mentioning that detailed research on energy and exergy is extremely important to better understand organic Rankine cycle processes and to mitigate environmental emissions, which has been fulfilled by the paper.

2. THERMODYNAMIC AND MATHEMATICAL MODELLING

Figure 1 (a), and 1 (b) represent schematic diagram, and T-S diagram of the organic Rankine cycle respectively. At first, the pump compresses the fluid from low to high pressure. Then, the

fluid goes into the evaporator and becomes heated and pressurized vapor by utilizing the thermal capacity of water that enters the expander. In the expander, it becomes low-pressure vapor and the generator produces electricity. After that, it enters the condenser and becomes a saturated liquid that passes to the pump. Finally, the continuation of the cycle occurs repeatedly.

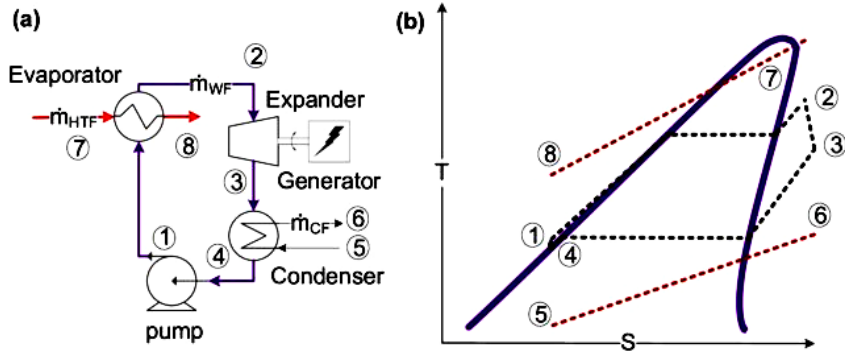


Figure 1. (a) Schematic diagram, and (b) T-S diagram of organic Rankine cycle [20]

$$\text{Mass Balance, } \frac{d\dot{m}_{cv}}{dt} = \sum_i \dot{m}_i - \sum_e \dot{m}_e \quad (1)$$

$$\text{Energy Balance, } \frac{dE_{cv}}{dt} = \dot{Q}_{cv} - \dot{W}_{cv} + \sum_i \dot{m}_i (h_i + \frac{V_i^2}{2} + gz_i) - \sum_e \dot{m}_e (h_e + \frac{V_e^2}{2} + gz_e) \quad (2)$$

$$\text{Exergy Balance, } \frac{dEx_{cv}}{dt} = \sum_i (1 - \frac{T_0}{T_j}) \dot{Q}_j - (\dot{W}_{cv} - P_0 \frac{dV_{cv}}{dt}) + \sum_i \dot{m}_i e_{fi} - \sum_e \dot{m}_e e_{fe} - \dot{E}_d \quad (3)$$

$$\text{Heat transfer rate in evaporator, } \dot{Q}_{ev} = \dot{m}_{HTF} (h_7 - h_8) = \dot{m}_{WF} (h_2 - h_1) \quad (4)$$

$$\text{Expander work, } \dot{W}_{exp} = \dot{m}_{WF} (h_2 - h_3) \eta_{exp} \quad (5)$$

$$\text{Heat transfer rate in condenser, } \dot{Q}_{co} = \dot{m}_{WF} (h_3 - h_4) = \dot{m}_{CF} (h_6 - h_5) \quad (6)$$

$$\text{Pump work, } \dot{W}_p = \frac{\dot{m}_{WF} (h_4 - h_1)}{\eta_p} \quad (7)$$

$$\text{Heat exergy from heat transfer fluid, } Ex_i = \dot{m}_{HTF} (e_{f7} - e_{f8}) = \dot{m}_{HTF} [(h_7 - h_8) - T_0 (s_7 - s_8)] \quad (8)$$

$$\text{Evaporator exergy balance, } E_{d,ev} = \dot{m}_{HTF} (e_{f7} - e_{f8}) + \dot{m}_{WF} (e_{f1} - e_{f2}) \quad (9)$$

$$\text{Second law efficiency of evaporator, } \eta_{II,ev} = \frac{\dot{m}_{WF} (e_{f2} - e_{f1})}{\dot{m}_{HTF} (e_{f7} - e_{f8})} \quad (10)$$

$$\text{Expander exergy balance, } E_{d,exp} = \dot{m}_{WF} (e_{f2} - e_{f3}) - \dot{W}_{exp} \quad (11)$$

$$\text{Second law efficiency of the expander, } \eta_{II,exp} = \frac{\dot{m}_{WF} (e_{f2} - e_{f3})}{\dot{W}_{exp}} \quad (12)$$

$$\text{Condenser exergy balance, } E_{d,co} = \dot{m}_{WF} (e_{f3} - e_{f4}) + \dot{m}_{CF} (e_{f5} - e_{f6}) \quad (13)$$

$$\text{Second law efficiency of condenser, } \eta_{II,co} = \frac{\dot{m}_{CF} (e_{f6} - e_{f5})}{\dot{m}_{HTF} (e_{f3} - e_{f4})} \quad (14)$$

$$\text{Pump exergy balance, } E_{d,p} = \dot{m}_{WF} (e_{f4} - e_{f1}) - \dot{W}_p \quad (15)$$

$$\text{Second law efficiency of pump, } \eta_{II,p} = \frac{\dot{m}_{WF} (e_{f4} - e_{f1})}{\dot{W}_p} \quad (16)$$

$$\text{Net work done for the overall system, } \dot{W}_{net} = \dot{W}_{exp} - \dot{W}_p \quad (17)$$

$$\text{Incoming heat exergy for the overall system, } \dot{q}_i = \dot{m}_{HHTF}(h_7 - h_8) \tag{18}$$

$$\text{Thermal efficiency or, first law efficiency for the overall system, } \eta_{I,sys} = \frac{\dot{W}_{net}}{\dot{q}_i} \tag{19}$$

$$\text{Second law efficiency for the overall system, } \eta_{II,sys} = \frac{\dot{W}_{net}}{\dot{E}_{x,i}} \tag{20}$$

3. OPERATING CONDITIONS AND THERMO-PHYSICAL PROPERTIES

All processes are assumed to be in steady-state, and the operation of all elements was performed under adiabatic conditions. Besides, thermal and pressure losses in the pipe have been neglected and the working fluid's condensing temperature is estimated to be 35° C.

Table 1 represents thermophysical properties of working fluids.

Table 1. Thermophysical properties of working fluids

Refrigerants	Critical Pressure (bar)	Critical Temperature (K)	Molar Mass (kg/mol)	Global Warming Potential
R21	51.81	451.48	0.102	151
R124	36.24	395.42	0.136	609
R141b	42.12	477.50	0.116	725
R245fa	36.51	427.01	0.134	1030
R1233zd(E)	35.70	438.75	0.130	0
R1234ze(Z)	35.33	423.27	0.114	0

Working fluids have been chosen based on the operational state, performance of the system, economy, and environmental consequences. Moreover, the chosen fluids can be sustained at higher temperatures. Therefore, choosing current working fluids instead of traditional fluids is very beneficial.

4. VALIDATION OF MODEL

Figures 2, 3, 4, and 5 compare mass flow rate, pump power, expander power, and heat available of refrigerant with O. Kaska [21], case-1 to validate the model. Results are within the acceptable range for all the mentioned figures. Figure 2 compares the mass flow rates of refrigerant, where the maximum difference was below 3%. Moreover, Figure 3 compares the pump power of refrigerant, where the maximum difference was under 5%. Besides, Figure 4 compares the expander power of refrigerant, where the maximum difference was below 4%. In addition, Figure 5 compares the heat available of refrigerant, where the maximum difference was under 5%.

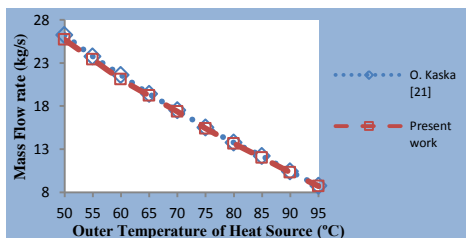


Figure 2. Comparison of mass flow rates of refrigerant

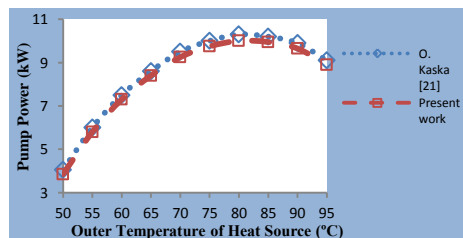


Figure 3. Comparison of pump power of refrigerant

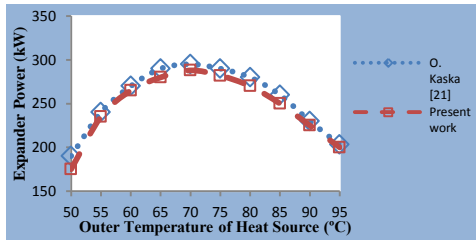


Figure 4. Comparison of expander power of refrigerant

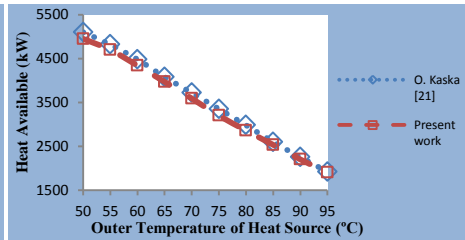


Figure 5. Comparison of heat available of refrigerant

5. RESULTS AND DISCUSSION

Relationship of net work output and evaporator pressure for selected refrigerants is shown in Figure 6. The saturation pressure of working fluids is responsible for variations of net work output. For all of the refrigerants, net work output increases with the increment of evaporator pressure. It has been observed that utilizing R124 refrigerant gives the lowest amount of net work output for all evaporator pressure. Moreover, it has been observed that for the lower values of evaporator pressures (from 10 to 40 bars), R141b refrigerant gives the highest amount of net work output. However, when evaporator pressure becomes more than 40 bars, R21 refrigerant gives the highest amount of net work output.

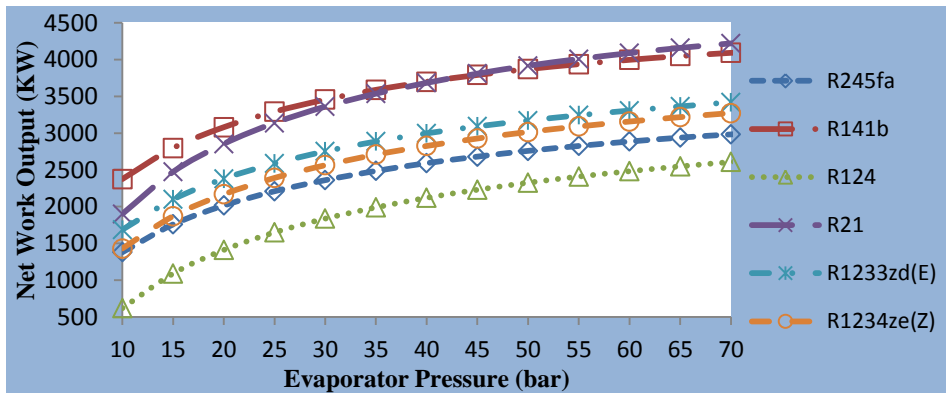


Figure 6. Relationship of net work output and evaporator pressure for selected refrigerants

Relationship of pump consumption and evaporator pressure for selected refrigerants is shown in Figure 7. Pump consumption is slightly affected by changing refrigerants. For all of the refrigerants, pump consumption increases with the increment of evaporator pressure. It has been observed that utilizing R124 refrigerant gives the lowest amount of pump consumption for the lower values of evaporator pressure. When evaporator pressure is more than 23 bars, R245fa gives the lowest value. Moreover, it has been observed that R141b refrigerant gives the highest amount of pump consumption for lower evaporator pressures whereas after evaporator pressure becomes more than 38 bars, R21 refrigerant gives the highest amount of pump consumption.

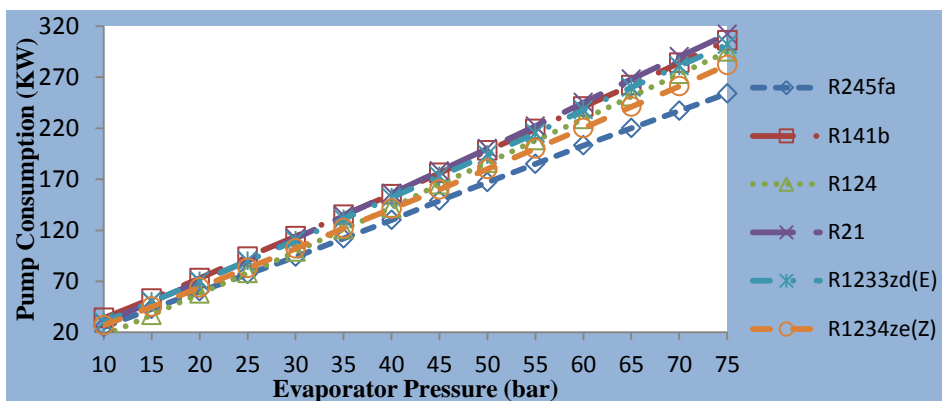


Figure 7. Relationship of pump consumption and evaporator pressure for selected refrigerants

Relationship of flow rates of coolant and evaporator pressure for selected refrigerants is shown in Figure 8. Heat rejection of the condenser is responsible for this variation. For all of the refrigerants, the flow rate of coolants decreases with the increment of evaporator pressure. R124 gives the highest amount of flow rate. Furthermore, R141b gives the lowest amount of flow rate for lower evaporator pressures but after evaporator pressure becomes more than 45 bars, R21 gives the lowest amount of flow rate.

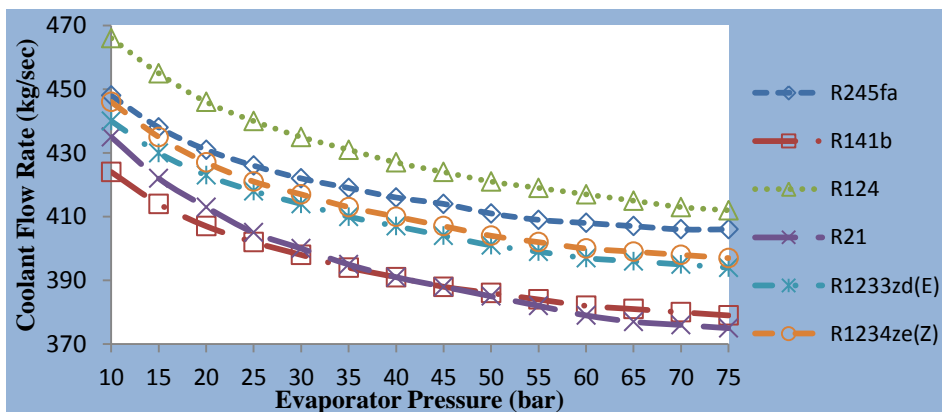


Figure 8. Relationship of flow rates of coolant and evaporator pressure for selected refrigerants

Relationship of thermal efficiency and evaporator pressure for selected refrigerants is shown in Figure 9. When the net work output is higher for the working fluid, the Organic Ranking cycle exhibits higher thermal efficiency. For all of the refrigerants, thermal efficiency increases with the increment of evaporator pressure. R124 gives the lowest amount of efficiency. Additionally, R141b gives the highest amount of efficiency for lower evaporator pressures but after evaporator pressure becomes more than 42 bars, R21 gives the highest amount of efficiency. Moreover, at a specific evaporator pressure, the pressure ratio varies from the refrigerant to refrigerant. At a low specific evaporator pressure, R124 and R141b give the lowest and the highest amount of pressure ratio respectively. So, efficiency increases with the increment of pressure ratio.

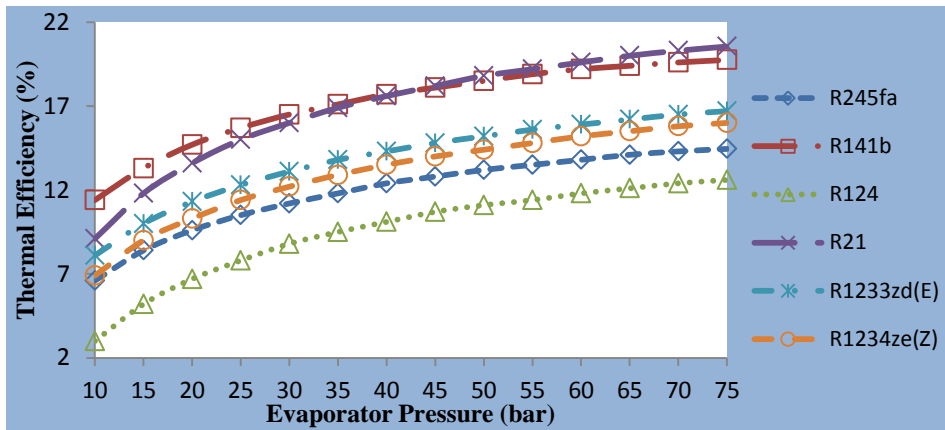


Figure 9. Relationship of thermal efficiency and evaporator pressure for selected refrigerants

Relationship of exergy efficiency and evaporator pressure for selected refrigerants is shown in Figure 10. When the net work output is higher for the working fluid, the Organic Rankine cycle exhibits higher exergy efficiency. For all of the refrigerants, exergy efficiency increases with the increment of evaporator pressure. R124 gives the lowest amount of efficiency. Additionally, R141b gives the highest amount of efficiency for lower evaporator pressures but after evaporator pressure becomes more than 42 bars, R21 gives the highest amount of efficiency.

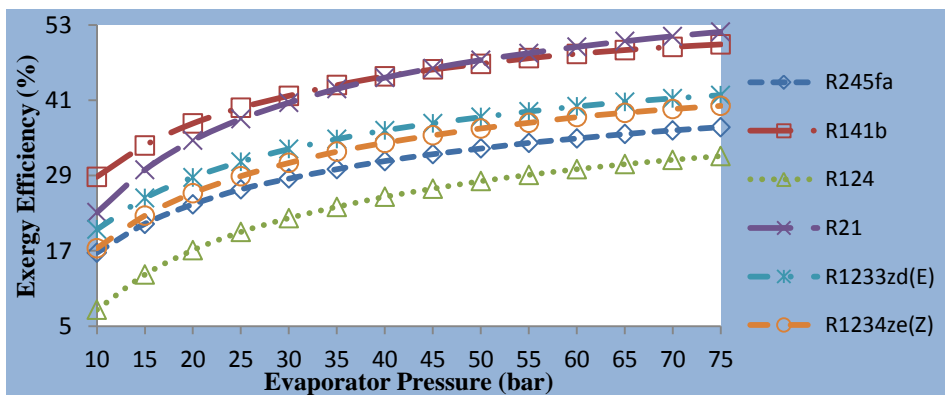


Figure 10. Relationship of exergy efficiency and evaporator pressure for selected refrigerants

Relationship of evaporator exergy destruction and evaporator pressure for selected refrigerants is shown in Figure 11. For all of the refrigerants, evaporator exergy destruction decreases with the increment of evaporator pressure. Here, R141b refrigerant gives the lowest amount of destruction and R21 refrigerant gives the highest amount of destruction.

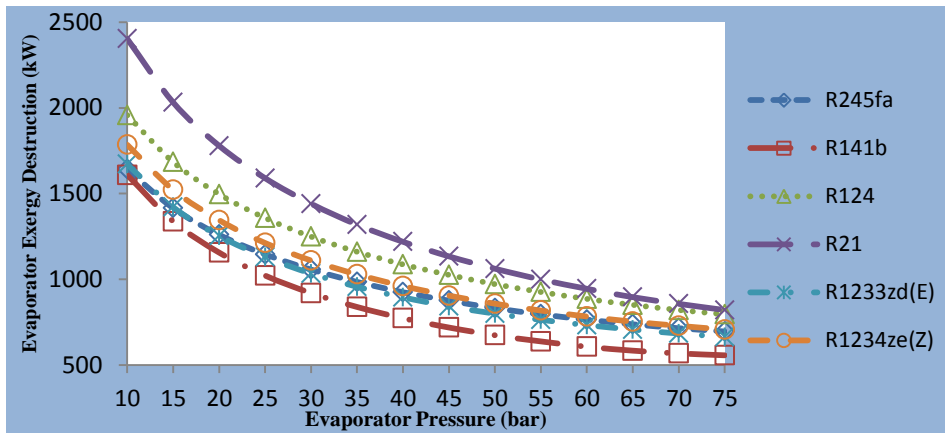


Figure 11. Relationship of evaporator exergy destruction and evaporator pressure for selected refrigerants

Relationship of expander exergy destruction and evaporator pressure for selected refrigerants is shown in Figure 12. For all of the refrigerants, expander exergy destruction increases with the increment of evaporator pressure. Here, R124 refrigerant gives the lowest amount of destruction. Moreover, R141b refrigerant gives the highest amount of destruction for lower evaporator pressure but after evaporator pressure becomes more than 30 bars, R21 gives the highest amount of destruction.

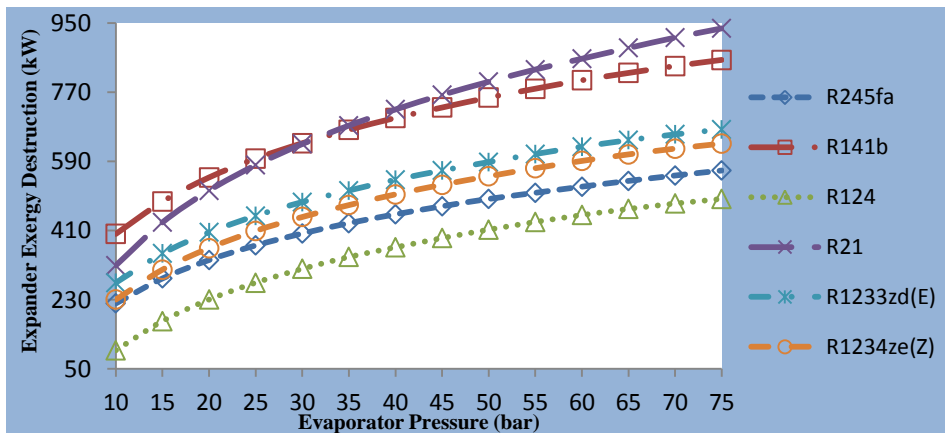


Figure 12. Relationship of expander exergy destruction and evaporator pressure for selected refrigerants

Relationship of condenser exergy destruction and evaporator pressure for selected refrigerants is shown in Figure 13. For all of the refrigerants, condenser exergy destruction decreases with the increment of evaporator pressure. Here, R21 refrigerant gives the lowest amount of destruction and R124 refrigerant gives the highest amount of destruction.

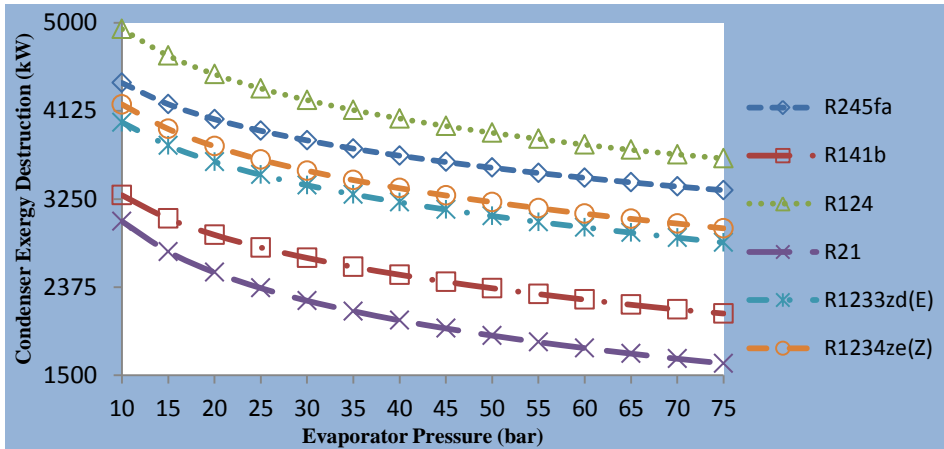


Figure 13. Relationship of condenser exergy destruction and evaporator pressure for selected refrigerants

Relationship of pump exergy destruction and evaporator pressure for selected refrigerants is shown in Figure 14. For all of the refrigerants, pump exergy destruction increases with the increment of evaporator pressure. Pump exergy destruction is slightly affected by changing refrigerants. Here, R124 refrigerant gives the lowest amount of destruction for lower evaporator pressure but after evaporator pressure becomes more than 20 bars, R245fa refrigerant gives the lowest amount of destruction. On the other hand, R141b refrigerant gives the highest amount of destruction for lower evaporator pressure but after evaporator pressure becomes more than 30 bars, R21 refrigerant gives the highest amount of destruction.

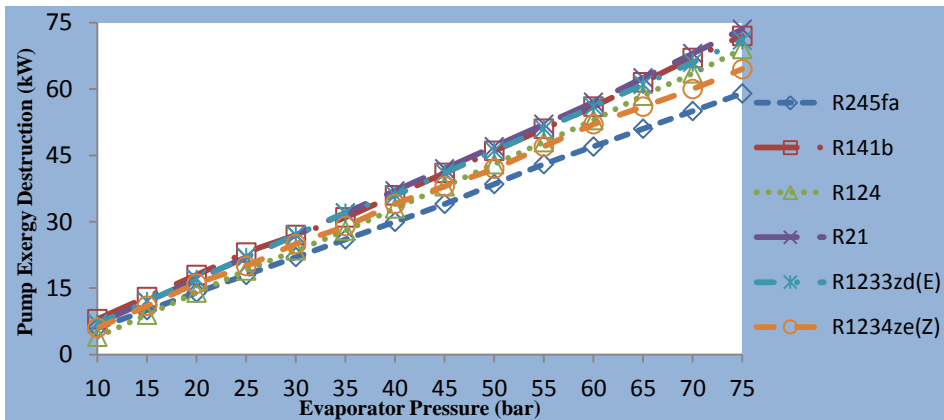


Figure 14. Relationship of pump exergy destruction and evaporator pressure for selected refrigerants

Relationship of condenser exergy rejection and evaporator pressure for selected refrigerants is shown in Figure 15. For all of the refrigerants, condenser exergy rejection decreases with the increment of evaporator pressure. Whenever evaporator pressure is increased, the decrement of the exit temperature of the expander occurs because of the expander's higher expansion. It

decreases the amount of condenser exergy rejection. Here, R21 refrigerant gives the lowest amount of rejection for lower evaporator pressure but when the evaporator pressure becomes more than 50 bars, R141b refrigerant gives the lowest amount of rejection. Additionally, R124 refrigerant gives the highest amount of rejection.

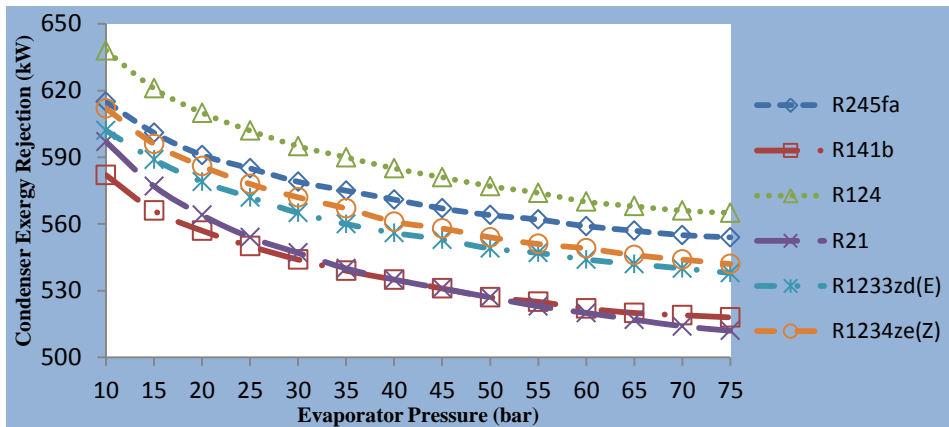


Figure 15. Relationship of condenser exergy rejection and evaporator pressure for selected refrigerants

Relationship of evaporator exergy efficiency and evaporator pressure for selected refrigerants is shown in Figure 16. For all of the refrigerants, evaporator exergy efficiency increases with the increment of evaporator pressure. Here, R21 refrigerant gives the lowest amount of efficiency and R141b refrigerant gives the highest amount of efficiency.

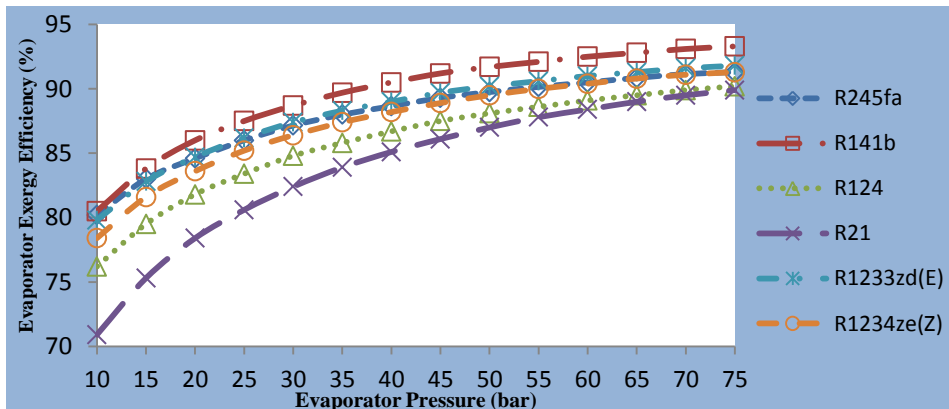


Figure 16. Relationship of evaporator exergy efficiency and evaporator pressure for selected refrigerants

Relationship of expander exergy efficiency and evaporator pressure for selected refrigerants is shown in Figure 17. For all of the refrigerants, expander exergy efficiency decreases with the increment of evaporator pressure. Here, R141b refrigerant gives the lowest amount of efficiency for evaporator pressure of 10 bars but when the evaporator pressure becomes more than 10 bars,

R21 refrigerant gives the lowest amount of efficiency. Moreover, R124 refrigerant gives the highest amount of efficiency.

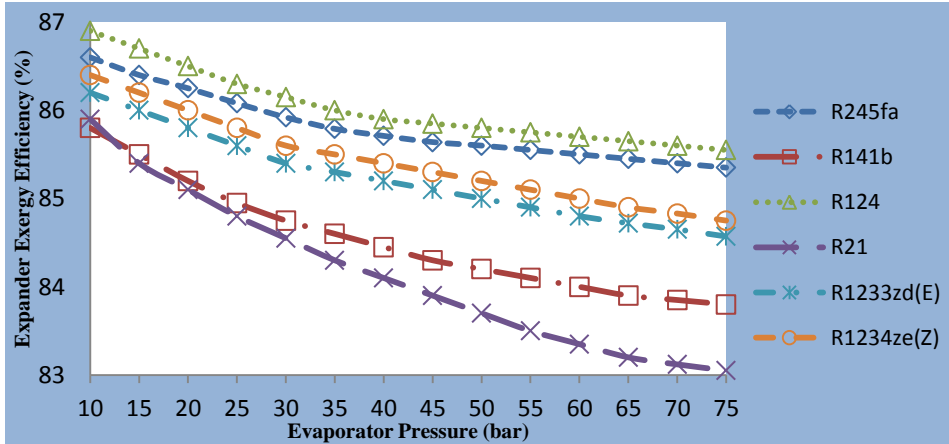


Figure 17. Relationship of expander exergy efficiency and evaporator pressure for selected refrigerants

Relationship of condenser exergy efficiency and evaporator pressure for selected refrigerants is shown in Figure 18. For all of the refrigerants, condenser exergy efficiency increases with the increment of evaporator pressure. Here, R124 refrigerant gives the lowest amount of efficiency and R21 refrigerant gives the highest amount of efficiency.

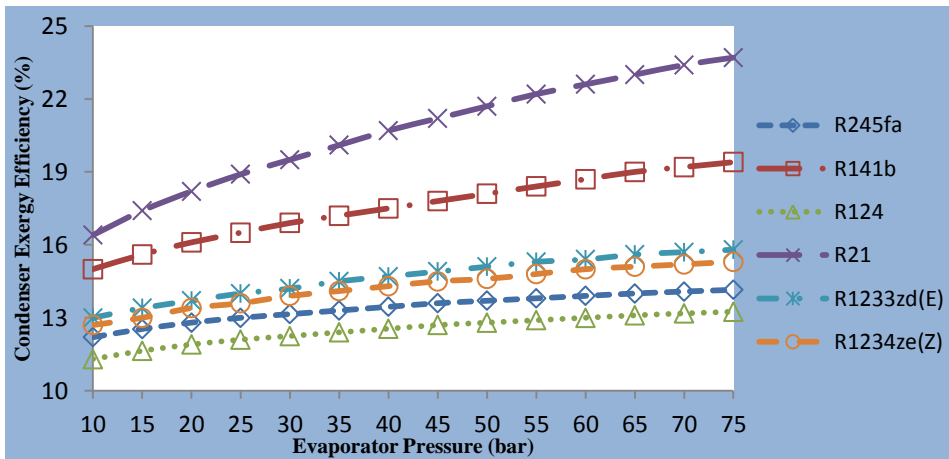


Figure 18. Relationship of condenser exergy efficiency and evaporator pressure for selected refrigerants

6. CONCLUSION

The organic Rankine cycle has been utilizing for investigating the exergy and energy of the waste heat recovery system. The findings of the paper can be summarized below:

1) Thermal efficiency increases with the increment of evaporator pressure for all of the chose refrigerants. R124 gives the lowest amount of thermal efficiency. R141b and R21 give the highest amount of thermal efficiency at low and high evaporator pressure respectively.

2) Exergy efficiency shows similar behavior like thermal efficiency. R124 gives the lowest amount of exergy efficiency. R141b and R21 give the highest amount of exergy efficiency at low and high evaporator pressure respectively.

3) Pump consumption and net work output increase with the increment of evaporator pressure. On the other hand, the coolant flow rate decreases with the increment of evaporator pressure. Moreover, R141b refrigerant gives the highest amount of pump consumption and net work output. On the contrary, R124 gives the highest amount of coolant flow rates.

4) Expander exergy destruction and pump exergy destruction increases with the increment of evaporator pressure. On the other hand, evaporator exergy destruction and condenser exergy destruction decrease with the increment of evaporator pressure. Moreover, R141b refrigerant gives the highest amount of expander and pump exergy destruction at low evaporator pressure but for high evaporator pressure, R21 refrigerant gives the highest amount of destruction. Additionally, R21 and R124 refrigerants give the highest amount of evaporator and condenser exergy destruction respectively.

5) Condenser exergy reduction decrease with the increment of evaporator pressure. R124 refrigerant gives the highest amount of reduction.

6) Evaporator and condenser exergy efficiency increase with the increment of evaporator pressure. On the other hand, expander exergy efficiency decreases with the increment of evaporator pressure. Moreover, R141b and R21 refrigerants give the highest amount of evaporator and condenser exergy efficiency respectively. On the contrary, R124 refrigerant gives the highest amount of expander exergy efficiency.

More environment-affable refrigerants can be analyzed in the future which could not be done in this paper due to the limitation of time.

NOMENCLATURE

<i>ORC</i>	Organic Rankine cycle
<i>LNG</i>	Liquefied natural gas
\dot{m}	Mass flow rate [kg/s]
<i>E</i>	Energy [J]
E_x	Exergy [J]
\dot{Q}	Heat transfer rate [J/s]
\dot{Q}_j	Heat transfer rate at instantaneous temperature T_j [J/s]
\dot{W}	Rate of work done [J/s]
<i>h</i>	Specific enthalpy [J/kg]
<i>V</i>	Velocity [m ³ /kg]
<i>gz</i>	Potential energy per unit mass [J/kg]
<i>T</i>	Temperature [°C or K]
T_o	Ambient temperature [°C or K]
P_o	Atmospheric pressure [Pa]
C_p	Specific heat capacity [J/°C]
η	Efficiency
<i>s</i>	Specific entropy [J/kg]
<i>S</i>	Total entropy [J]
e_f	Specific flow exergy [J/kg]

Subscript

<i>cv</i>	Control volume
<i>i</i>	Inlet
<i>e</i>	Exit
<i>HTF</i>	Heat transfer fluid
<i>p</i>	Pump
<i>exp</i>	Expander
<i>ev</i>	Evaporator
<i>co</i>	Condenser
<i>WF</i>	Working fluid
<i>CF</i>	Cooling fluid
<i>s</i>	Isentropic value
<i>d</i>	Distruction
<i>sys</i>	System

REFERENCES

- [1] F. Yang, H. Zhang, C. Bei, S. Song, and E. Wang, "Parametric optimization and performance analysis of ORC (organic Rankine cycle) for diesel engine waste heat recovery with a fin-and-tube evaporator," *Energy*, vol. 91, pp. 128-141, 2015, doi: <https://doi.org/10.1016/j.energy.2015.08.034>.
- [2] N. Nazari, P. Heidarnajad, and S. Porkhial, "Multi-objective optimization of a combined steam-organic Rankine cycle based on exergy and exergo-economic analysis for waste heat recovery application", *Energy conversion and management*, vol. 127, pp. 366-379, 2016, doi: [10.1016/j.enconman.2016.09.022](https://doi.org/10.1016/j.enconman.2016.09.022).
- [3] H. Yağlı, Y. Koç, A. Koç, A. Görgülü, and A. Tandiroğlu, "Parametric optimization and exergetic analysis comparison of subcritical and supercritical organic Rankine cycle (ORC) for biogas fuelled combined heat and power (CHP) engine exhaust gas waste heat," *Energy*, vol. 111, pp. 923-932, 2016, doi: [10.1016/j.energy.2016.05.119](https://doi.org/10.1016/j.energy.2016.05.119).
- [4] H. Zhai, Q. An, L. Shi, V. Lemort, and S. Quoilin, "Categorization and analysis of heat sources for organic Rankine cycle systems," *Renewable and Sustainable Energy Reviews*, vol. 64, pp. 790-805, 2016, doi: [10.1016/j.rser.2016.06.076](https://doi.org/10.1016/j.rser.2016.06.076).
- [5] W. Sun, X. Yue, and Y. Wang, "Exergy efficiency analysis of ORC (Organic Rankine Cycle) and ORC-based combined cycles driven by low-temperature waste heat," *Energy Conversion and Management*, vol. 135, pp. 63-73, 2017, doi: [10.1016/j.enconman.2016.12.042](https://doi.org/10.1016/j.enconman.2016.12.042).
- [6] H. Tian, L. Chang, Y. Gao, G. Shu, M. Zhao, and N. Yan, "Thermo-economic analysis of zeotropic mixtures based on siloxanes for engine waste heat recovery using a dual-loop organic Rankine cycle (DORC)," *Energy conversion and management*, vol. 136, pp. 11-26, 2017, doi: [10.1016/j.enconman.2016.12.066](https://doi.org/10.1016/j.enconman.2016.12.066).
- [7] T. Koroglu, "Advanced exergy analysis of an organic Rankine cycle waste heat recovery system of a marine power plant," *Journal of Thermal Engineering*, vol. 3, no. 2, pp. 1136-1148, 2017, doi: [10.18186/thermal.298614](https://doi.org/10.18186/thermal.298614).
- [8] S. Seyedkavoosi, S. Javan, and K. Kota, "Exergy-based optimization of an organic Rankine cycle (ORC) for waste heat recovery from an internal combustion engine (ICE)," *Applied Thermal Engineering*, vol. 126, pp. 447-457, 2017, doi: [j.applthermaleng.2017.07.124](https://doi.org/10.1016/j.applthermaleng.2017.07.124).
- [9] Z. Ge, J. Li, Q. Liu, Y. Duan, and Z. Yang, "Thermodynamic analysis of dual-loop organic Rankine cycle using zeotropic mixtures for internal combustion engine waste heat recovery," *Energy conversion and management*, vol. 166, pp. 201-214, 2018, doi: [10.1016/j.enconman.2018.04.027](https://doi.org/10.1016/j.enconman.2018.04.027).

- [10] Y. Koç, H. Yağlı, and A. Koç, "Exergy analysis and performance improvement of a subcritical/supercritical organic rankine cycle (ORC) for exhaust gas waste heat recovery in a biogas fuelled combined heat and power (CHP) engine through the use of regeneration," *Energies*, vol. 12, no. 4, p. 575, 2019, doi: 10.3390/en12040575.
- [11] H. Khosravi, G. R. Salehi, and M. T. Azad, "Design of structure and optimization of organic Rankine cycle for heat recovery from gas expander: The use of 4E, advanced exergy and advanced exergoeconomic analysis," *Applied Thermal Engineering*, vol. 147, pp. 272-290, 2019, doi: <https://doi.org/10.1016/j.applthermaleng.2018.09.128>.
- [12] Y. Liang, X. Bian, W. Qian, M. Pan, Z. Ban, and Z. Yu, "Theoretical analysis of a regenerative supercritical carbon dioxide Brayton cycle/organic Rankine cycle dual loop for waste heat recovery of a diesel/natural gas dual-fuel engine," *Energy Conversion and Management*, vol. 197, p. 111845, 2019, doi: 10.1016/j.enconman.2019.111845.
- [13] F. Han, Z. Wang, Y. Ji, W. Li, and B. Sundén, "Energy analysis and multi-objective optimization of waste heat and cold energy recovery process in LNG-fueled vessels based on a triple organic Rankine cycle," *Energy Conversion and Management*, vol. 195, pp. 561-572, 2019, doi: 10.1016/j.enconman.2019.05.040.
- [14] X. Liu, X. Yang, M. Yu, W. Zhang, Y. Wang, P. Cui, Z. Zhu, Y. Ma, and J. Gao, "Energy, exergy, economic and environmental (4E) analysis of an integrated process combining CO₂ capture and storage, an organic Rankine cycle and an absorption refrigeration cycle," *Energy Conversion and Management*, vol. 210, p. 112738, 2020, doi: 10.1016/j.enconman.2020.112738.
- [15] G. Liao, E. Jiaqiang, F. Zhang, J. Chen, and E. Leng, "Advanced exergy analysis for Organic Rankine Cycle-based layout to recover waste heat of flue gas," *Applied Energy*, vol. 266, p. 114891, 2020, doi: 10.1016/j.apenergy.2020.114891.
- [16] Z. Hou, X. Wei, X. Ma, and X. Meng, "Exergoeconomic evaluation of waste heat power generation project employing organic Rankine cycle," *Journal of Cleaner Production*, vol. 246, p. 119064, 2020, doi: <https://doi.org/10.1016/j.jclepro.2019.119064>.
- [17] G. Valencia Ochoa, C. Isaza-Roldan, and J. D. Forero, "Economic and Exergo-Advance Analysis of a Waste Heat Recovery System Based on Regenerative Organic Rankine Cycle under Organic Fluids with Low Global Warming Potential," *Energies*, vol. 13, no. 6, p. 1317, 2020, doi: 10.3390/en13061317.
- [18] S. Wang, W. Zhang, Y.Q. Feng, X. Wang, Q. Wang, Y. Z. Liu, Y. Wang, and L. Yao, "Entropy, Entropy and Exergy Analysis of a Dual-Loop Organic Rankine Cycle (DORC) Using Mixture Working Fluids for Engine Waste Heat Recovery," *Energies*, vol. 13, no. 6, p. 1301, 2020, doi: 10.3390/en13061301.
- [19] X. Zhou, P. Cui, and W. Zhang, "Thermal and Exergy Analysis of an Organic Rankine Cycle Power Generation System with Refrigerant R245fa," *Heat Transfer Engineering*, vol. 41, no. 9-10, pp. 905-918, 2020, doi: 10.1080/01457632.2019.1576824.
- [20] S. Lecompte, H. Huisseune, M. V. D. Broek, B. Vanslambrouck, and M. D. Paepe, "Review of organic Rankine cycle (ORC) architectures for waste heat recovery," *Renewable and sustainable energy reviews*, vol. 47, pp. 448-461, 2015, doi: 10.1016/j.rser.2015.03.089.
- [21] O. Kaska, "Energy and exergy analysis of an organic Rankine for power generation from waste heat recovery in steel industry", *Energy Conversion and Management*, vol. 77, pp. 108-117, 2014, doi: 10.1016/j.enconman.2013.09.026.